



Hydrodynamic modeling to predict the thickness of boundary layer of a membrane vertically immersed in a bioreactor

Amir Ali Poostchi^{a,b,*}, Mostafa Hosseinzadeh^c

^aPetrochemical Industries Development Management Company, Tehran, Iran, Tel. +98 (21) 88843177; Fax: +98 (21) 88848133; emails: poostchi@pidmco.ir, apoostchi@ut.ac.ir

^bPersian Gulf Petrochemical Industry Company, P.O. Box 15858–49568, Tehran, Iran

^cDepartment of Chemical Engineering, Iran University of Science and Technology, Tehran, Iran, mhoseinzadeh@chemeng.iust.ac.ir

Received 20 June 2016; Accepted 3 December 2016

ABSTRACT

The mathematical modeling was developed on the basis of continuity and momentum relationships over the porous medium that has been derived to estimate the thickness of hydrodynamic boundary layer, extended along the surface of membrane submerged in bioreactor. The flow regime was approximated to be laminar at the close proximity to membrane surface. In the current modeling, two coordinates of velocity, namely in x - and y -directions, have been applied for the derivation of governing equation of convective momentum transfer. The permeate flux passing through the membrane medium was assumed to create the perpendicular velocity profile in y -direction while the gas introduced into the bioreactor has created the velocity profile in x -direction at the adjacent periphery of membrane medium. The results obtained from the solution of the derived model demonstrated that the interfacial gas velocity strictly influenced the height of hydrodynamic boundary layer. The height of boundary layer ranged from 0.9 to 4.5 mm as the interfacial gas velocity varied from 0.1 to 2 m s⁻¹. The model presented that the height of the boundary layer increased when the interfacial gas velocity decreased. The results also revealed that the increase in the permeate flux was caused due to the decrease in the height of laminar boundary layer, however, the rate of increase in the height of boundary layer decreased when the permeate velocity increased.

Keywords: Membrane bioreactor; Boundary layer; Hydrodynamic modeling

1. Introduction

The majority of publications relevant to membrane bioreactor (MBR) have been focusing on the feasible–applicable protocols for the purpose of minimization of fouling formed on membrane surface [1–7]. The intermittent aeration and air scouring have mostly been known as the operational solution to hinder the formation of fouling in MBRs [8,9]. Since, the hydrodynamic interactions could influence the qualitative and quantitative performances of MBRs, so the hydrodynamic behavior of multi-phase, gas–liquid–solid, must be recognized specifically at the front zone closed to the surface of membrane. Very few studies have precisely

been conducted to determine the hydrodynamic behavior as well as the boundary layer; however, most studies have been carried out on content of the concentration boundary layer formed next to membrane surface [10,11]. Notwithstanding the significance of the hydrodynamic boundary layer upon a flat sheet membrane, the existing correlations had still been derived based on assumptions and conditions applicable to the fluid flowing over an impermeable flat plate [12]. Therefore, permeability of a flat sheet membrane makes no allowance as an independent parameter principally influencing the hydrodynamic boundary layer. Hosseinzadeh et al. [13] indicated that the aeration and permeate flux made major changes on cake formation upon membrane surface. The shear stress enhancement on the membrane surface

* Corresponding author.

increased the permeate flux [14]. The membrane fouling reduced with higher aeration due to increasing shear stress at the membrane surface [15]. The drag force acted on the cake layer could prevail upon the shear stress generated by the aeration [16]. In fact, the membrane surface environs where change in the velocity and the shear rate happened was known as the boundary layer; aeration and permeate flow have impressed in. Thus, the height of the laminar hydrodynamic boundary layer could be related to the thickness of cake layer formed on membrane surface during solid–liquid separation process. This study presented a newly developed approach in mathematical modeling obtained from the combination of continuity, convective momentum and surface force equations to estimate the laminar boundary layer thickness as a function of aeration intensity, creating the velocity profile along the membrane surface, and permeability flow rate, creating the velocity profile perpendicular to membrane surface. This modeling could also be incorporated into the mechanisms of dynamic membrane and/or fouling layer formation.

2. Mathematical modeling

In the early works related to the hydrodynamic behavior in a submerged membrane bioreactor, the thickness of boundary layer has been calculated using Carman–Kozeny correlation applied for a flat plate in the state of laminar flow. In this modeling, vertically submerged membrane could be simulated to a permeable flat plate where the filtrate passed through the porous media, so called the membrane [17]. The typical schematic diagram of a flat sheet membrane with the relative velocity coordination is depicted in Fig. 1.

The x -coordinate was measured from the leading edge of the flat sheet membrane, and y -coordinate was measured normal to the membrane surface. The corresponding velocity components were V_x and V_y in the x - and y -directions, respectively. The permeable velocity passing through the membrane, V_{y0} , that was calculated by multiplication of permeate flux, J , to cross-sectional area of membrane, A , was assumed to be uniform flow stream and arranged in a normal line to free stream velocity, $V_{x\infty}$, in the bioreactor. It was also assumed that the magnitude of permeable velocity near porous membrane medium had no significant changes to the

inviscid flow field created by aeration outside the boundary layer. The flow regime created by aeration intensity throughout the bioreactor was considered as a laminar pattern. The Reynolds number was:

$$Re = \rho V_y d_h / \mu \tag{1}$$

where μ was fluid viscosity, and d_h is the hydraulic diameter. Pontoni et al. [18] showed the characteristics of sludge produced by MBR and conventional activated sludge (CAS) was different. Khalili-Garakani et al. [19] developed a correlation for calculation of the apparent viscosity of activated sludge in MBR as follows:

$$\mu = 0.0286 MLSS^{1.5} U_g^{-1} \exp(-7.7 / R_g T) \tag{2}$$

Also, d_h was defined as follows [20]:

$$d_h = 4A_c / P_w \tag{3}$$

The Reynolds number was roughly obtained 155, which was in the range of laminar flow pattern at normal and operational condition in MBRs, mixed liquor suspended solids (MLSS) of 8 g/L, U_g of 0.5 m³/h.m², and V_y of 1 m/s [21]. Therefore, the Reynolds number was approximated as high as enough for boundary layer assumptions to be applicable for a membrane planar [22,23].

The schematic boundary layer formed close to the surface of vertically submerged membrane was also demonstrated in Fig. 1. The control volume considered in boundary layer was unit depth and bounded in the xy plane with Δx in length and Δy in width. The force equation in x -direction incorporated into the specified element in boundary layer was expressed as follows:

$$\sum F_x = \iint_{C.S} \rho V_x (\hat{V} \cdot \hat{n}) dA + \frac{\partial}{\partial t} \iiint_{C.V} \rho V_x dV \tag{4}$$

The second term of right-hand side of Eq. (4) became null for steady-state condition. The left-hand side of Eq. (4) could be extended as the dynamic pressure, gravity and shear stress forces incorporated into the x -direction of defined control volume, and it could be written as follows:

$$\sum F_x = P\delta|_x - P\delta|_{x+\Delta x} + \frac{P\delta|_x + P\delta|_{x+\Delta x}}{2} (\delta|_{x+\Delta x} - \delta|_x) - \tau_0 \Delta x \tag{5}$$

where δ represented the boundary layer thickness and P (defined as $P = p - \rho gz$, in which the term p is the static pressure) is the modified pressure, the sum of the pressure and gravitational terms, and also the body forces could be neglected. By combining Eqs. (4) and (5), the following equation could be written as follows:

$$-\delta \frac{dP}{dx} = \tau_0 + V_\infty V_{y0} + \frac{d}{dx} \int_0^\delta \rho V_x^2 dy - V_\infty \frac{d}{dx} \int_0^\delta \rho V_x dy \tag{6}$$

where τ_0 was the shear stress involved in the membrane surface and defined as:

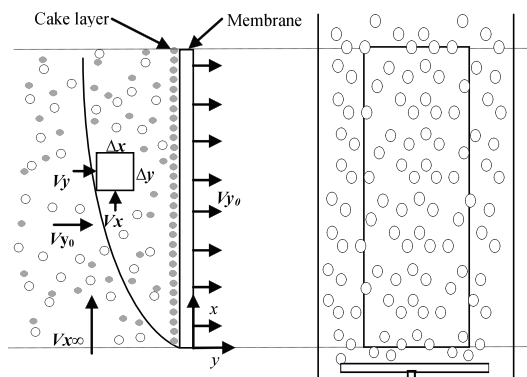


Fig. 1. Schematic diagram of vertically immersed membrane in the bioreactor with respect to the boundary layer.

$$\tau_0 = \mu \frac{dV_x}{dy} = \mu \frac{V_\infty}{\delta} \quad (7)$$

The boundary layer concept assumed the inviscid flow in the external surface of the boundary layer and Bernoulli's equation could be written as follows:

$$\delta \frac{dP}{dx} = \frac{d}{dx} (\delta V_\infty^2) - V_\infty \frac{d}{dx} (\delta V_\infty) \quad (8)$$

The left-hand sides of Eqs. (6) and (8) are similar. Thus, the right-hand sides could be related with proper rearrangement as in the following form:

$$\frac{\tau_0}{\rho} + \frac{V_\infty V_{y0}}{\rho} = \left(\frac{dV_\infty}{dx} \right) \int_0^\delta (V_\infty - V_x) dy + \frac{d}{dx} \int_0^\delta V_x (V_\infty - V_x) dy \quad (9)$$

Eq. (6) is the modified form of the von Karman momentum integral expression. The term $\frac{V_\infty V_{y0}}{\rho}$ demonstrated in Eq. (9) is the modification index of the Karman's expression for permeable medium such as membrane and considered as the distinction criterion of boundary layer's integral expressions for the permeable and impermeable flat plate. In order to investigate the effect of different velocity profiles on the thickness boundary layer formed upon the membrane surface, the three different linear, polynomial and sinuous profiles were assumed as follows, respectively [23]:

$$\frac{V_x}{V_\infty} = \frac{y}{\delta} \quad (10)$$

$$\frac{V_x}{V_\infty} = 1.5 \left(\frac{y}{\delta} \right) - 0.5 \left(\frac{y}{\delta} \right)^3 \quad (11)$$

$$\frac{V_x}{V_\infty} = \sin \left(\frac{\pi y}{2\delta} \right) \quad (12)$$

3. Results and discussion

The hydrodynamic boundary layer was derived for a membrane with the length 10 cm submerged in a bioreactor. The membrane surface aeration was named specific aeration demand (SAD), with respect to either the membrane area (SAD_m) or permeate flow (SAD_p). For the flat sheet membranes, SAD_m was 0.34–0.75 m³ (air)/h.m² (membrane surface) and SAD_p is 20–90 m³ (air)/m³ (filtered flow). The membrane permeate flux was called LMH and 8–62 L/h.m² (membrane surface) [21]. Therefore, permeate velocity was 2×10^{-6} – 20×10^{-6} m/s. The air as gas phase was introduced through the pipe distributors mounted at the bottom of bioreactor. It was assumed that the bulk velocity throughout the volume of the bioreactor was equal to bubble velocity. The gas velocity was considered in the range of 0.1–2 m/s. This range was the conventional and operational for aeration intensity in MBR processes. The range of velocity in *y*-direction was provided based on the practical permeate flux reported in the recent studies related to MBRs. To compare the three proposed velocity profiles, the corresponding plots were drawn in Fig. 2. The plots for two profiles including sinuous

and polynomial displayed the same trend with no significant deviation. The variations of the thickness of the boundary layer against the length of membrane were shown in Fig. 3 for three velocity profiles. As depicted, all plots followed the same trend, and the height of the boundary layer increased when increasing the length of membrane. It was also demonstrated that the variation of boundary layer thickness for sinuous and polynomial profiles were somewhat closed together as compared with the linear profile. As depicted in Figs. 2 and 3, although the velocity profiles for sinuous and polynomial became more close to each other, however, the plots of variations of height of boundary layer for these two were less close together. It could be explained that in Fig. 2 the state of Eqs. (10) and (11) for variable *y*/ δ was the same when Taylor series was developed. In Fig. 3, the slope of both polynomial and sinuous equation was similar at low values of *x* and δ variable. By increasing *y*/ δ parameter, sinuous equation reached an inflection point when *y* value became equal to δ . In physical boundary layer, no inflection point was probably observed in real case. Thus, polynomial state could predict better as compared with sinuous equation.

Fig. 4 displayed the variations of height of boundary layer at several aeration intensities. Similarly, plots had a general same trend, and the rate of variations for lower aeration intensities was sharper as compared with higher aerations. It also obtained

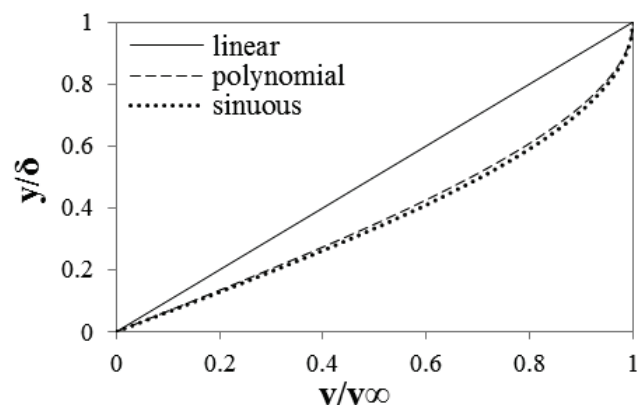


Fig. 2. Three different velocity profiles.

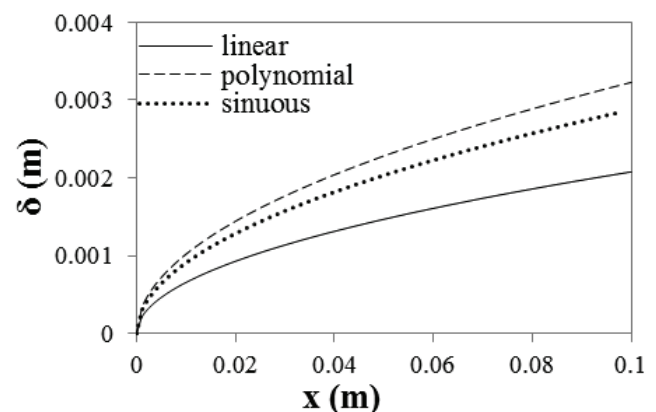


Fig. 3. The variations of the thickness of the boundary layer against the length of membrane for three velocity profile.

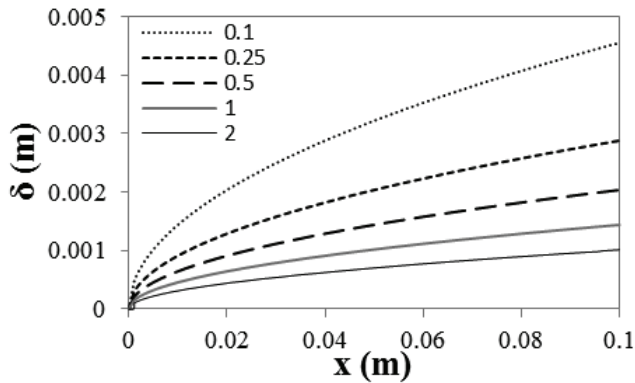


Fig. 4. The variations of height of boundary layer at several aeration intensities (V_{∞}): 0.1 (...), 0.25 (- - -), 0.5 (- · - ·), 1 (-) and 2 (- - -) m/s.

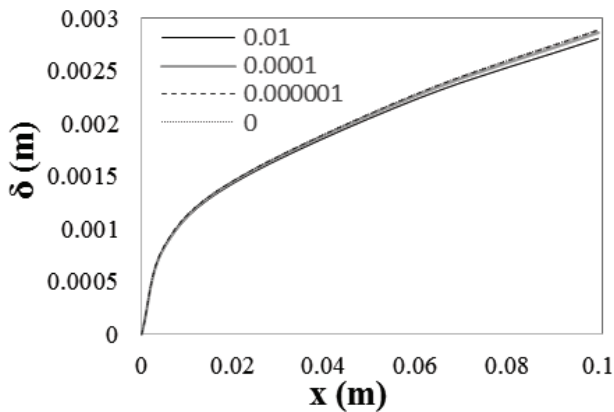


Fig. 5. The variations of height of boundary layer at different permeate velocities (V_p): 0 (...), 0.000001 (- · - ·), 0.0001 (-) and 0.01 (- - -) m/s.

that at the higher ranges of aeration, the height of boundary layer reached steady state sooner than lower ranges, along membrane. It could imply a fact that the stability of the cake layer formed on membrane in the terms of higher ranges of aeration was more difficult than the lower ranges of aeration. Fig. 5 depicted the variations of height of boundary layer at several permeate velocities passing through the membrane medium. As could be seen, the height of boundary layer slightly increased while decreasing permeate velocity. It meant that when the length of membrane became higher the effect of permeate velocity on the height of boundary layer was more tangible.

4. Conclusions

The new approach of hydrodynamic modeling for membrane vertically submerged in a bioreactor has been developed. The effect of aeration intensity, permeate velocity at three different velocity profiles, namely linear, polynomial, and sinusoidal, on the height of boundary layer were investigated. The results obtained from modeling while increasing the interfacial gas velocity the height of boundary layer decreased. The height of hydrodynamic boundary layer was varied between 0.9 and 4.5 mm at the upper edge of membrane. The derived model also presented that when the

permeate velocity increased the height of boundary layer increased, thus causing the deposition of particulate matters upon membrane surface. The results obtained from the model showed that the height of boundary layer was utmost value when membrane acted as impermeable plate. It meant that the term $\frac{V_{\infty} V_{y0}}{\rho}$ in the derived model could play important role to predict the height of boundary layer in permeable plates such as membrane submerged in a bioreactor.

Symbols

A	—	Area, m ²
d	—	Diameter, m
J	—	Permeate flux, L/m ² /h (LMH)
MLSS	—	Mixed liquor suspended solids, g/L
P	—	Pressure, Pa
P_w	—	Wetted perimeter, m
R_g	—	Universal gas constant, J/K.mol
T^g	—	Temperature, K
t	—	Time, s
U_g	—	Aeration intensity, m ³ (air)/s.m ² (membrane area)
V	—	Velocity, m/s
δ	—	Height of boundary layer, m
μ	—	Viscosity, kg/m.s
ρ	—	Density, kg/m ³
τ	—	Shear stress, Pa

References

- [1] J. Wu, P. Le-Clech, Novel filtration mode for fouling limitation in membrane bioreactors, *Water Res.*, 24 (2008) 1–8.
- [2] D. Jeison, J.B. Van Lier, Cake layer formation in anaerobic submerged membrane bioreactors (AnSMBR) for wastewater treatment, *J. Membr. Sci.*, 284 (2006) 277–236.
- [3] Z. Ying, G. Ping, Effect of powdered activated carbon dosage on retarding membrane fouling in MBR, *Sep. Purif. Technol.*, 52 (2006) 154–160.
- [4] B. Marrot, A. Barrios-Martinez, P. Moulin, Biodegradation of high phenol concentration by activated sludge in an immersed membrane bioreactor, *Biochem. Eng. J.*, 85 (2006) 174–183.
- [5] M. Kim, G. Nakhla, Comparative studies on membrane fouling between two membrane-based biological nutrient removal systems, *J. Membr. Sci.*, 331 (2009) 91–99.
- [6] J.S. Baker, L.Y. Dudley, Biofouling in membrane systems – a review, *Desalination*, 118 (1998) 81–90.
- [7] X.M. Wang, X.Y. Li, Accumulation of biopolymer clusters in a submerged membrane bioreactor and its effect on membrane fouling, *Water Res.*, 42 (2008) 855–862.
- [8] C.Y. Chang, J.S. Chang, Y.W. Lin, Quantification of air stripping and biodegradation of organic removal in acrylonitrile-butadiene-styrene (ABS) industry wastewater during submerged membrane bioreactor operation, *Desalination*, 191 (2006) 162–168.
- [9] S. Judd, The status of membrane bioreactor technology, *Trends Biotechnol.*, 26 (2008) 109–116.
- [10] F. Zhang, W. Jing, W. Xing, Modeling of cross-flow filtration processes in an airlift ceramic membrane reactor, *J. Ind. Eng. Chem. Res.*, 48 (2009) 10637–10642.
- [11] T.W. Cheng, Modified boundary layer resistance model for membrane ultrafiltration, *J. Sci. Eng.*, 4 (2001) 111–117.
- [12] Y. Mao-Sheng, Z. Han-Min, Y. Feng-Lin, Experimental study on application of the boundary layer theory for estimating steady aeration intensity of pre-coated dynamic membrane bioreactors, *Desalination*, 230 (2008) 100–112.
- [13] M. Hosseinzadeh, M.R. Mehrnia, N. Mostoufi, Experimental study and modeling of fouling in immersed membrane

- bioreactor operating in constant pressure filtration, *Math. Prob. Eng.*, 2013 (2013) 1–7.
- [14] N.V. Ndinisa, A.G. Fane, D.E. Wiley, D.F. Fletcher, Fouling control in a submerged flat sheet membrane system: Part II—Two-phase flow characterization and CFD simulations, *Sep. Sci. Technol.*, 41 (2005) 1411–1445.
- [15] M.S. Amirafabi, N. Mostoufi, M. Hosseinzadeh, M.R. Mehrnia, Reduction of membrane fouling by innovative method (injection of air jet), *J. Environ. Health Sci. Eng.*, 12 (2014) 1–8.
- [16] G. Belfort, R.H. Davis, The behavior of suspensions and macromolecular solutions, in cross-flow microfiltration, *J. Membr. Sci.*, 96 (1994) 1–58.
- [17] O. Aydın, A. Kaya, Laminar boundary layer flow over a horizontal permeable flat plate, *Appl. Math. Comput.*, 161 (2005) 229–240.
- [18] L. Pontoni, M. Fabbicino, L. Frunzo, F. Pirozzi, G. Esposito, Biological stability and dewaterability of CAS and MBR sludge, *Desal. Wat. Treat.*, 57 (2016) 22926–22933.
- [19] A.H. Khalili-Garakani, N. Mostoufi, F. Sadeghi, M. Hosseinzadeh, H. Fatourehchi, M.H. Sarrafzadeh, M.R. Mehrnia, Comparison between different models for rheological characterization of activated sludge, *Iran. J. Environ. Health Sci. Eng.*, 8 (2011) 255–264.
- [20] S.J. Ergas, D.E. Rheinheimer, Drinking water denitrification using a membrane bioreactor, *Water Res.*, 38 (2004) 3225–3232.
- [21] S. Judd, *The MBR Book: Principles and Applications of Membrane Bioreactors in Water and Wastewater Treatment*, 1st ed., Elsevier, Amsterdam, 2006.
- [22] H. Schlichting, *Boundary-Layer Theory*, 6th ed., McGraw-Hill, New York, 1968.
- [23] R.B. Bird, W.E. Stewart, E.N. Lightfoot, *Transport Phenomena*, 2nd ed., Wiley, New York, 2002.